

Finite element analyses of soil-structure interaction in masonry arch bridges

J. Wang and C. Melbourne

School of Computing, Science and Engineering, University of Salford, Salford, Greater Manchester M5 4WT, UK

ABSTRACT: Two finite element models are created using a commercially available finite element package: a simple soil-arch interaction model and a full bridge model. The simple soil-arch interaction model is mainly used for parametric studies within the service loading range. The material for both arch and soil in the simple soil-arch model is assumed to be within its elastic limit and the interface between the arch and soil is characterised as a friction contact interface. The full bridge model, however, has been created for predicting the failure of the same corresponding experiment. In the full bridge model, the smeared cracking approach is adopted for modelling the masonry behaviour, while the nonlinear behaviour of the soil is simulated with a Drucker-Prager material model. The same friction contact interface is adopted for the full bridge mode. The full bridge model is capable of reproducing the essential features observed in full scale experiments

1 INTRODUCTION

In the past decades comprehensive research has been carried out on masonry arch bridges. However, the performance of the backfill has generally not been the focal point and only a very limited range of fill types have been tested to date. Additionally, rigid abutments have been adopted in most laboratory tests which are less representative to those found in practice. Although it is well accepted that soil-arch interaction has a significant influence on the load carrying capacity of many masonry arch bridges, the complex nature of the soil-arch interaction is not well understood.

The work reported in this paper is part of the study of soil-structure interaction in masonry arch bridges. An experimental programme comprising tests on a series of 3m span masonry arches between movable abutments and with different backfill is currently ongoing and the new purpose-built large-scale plane-strain test rig enables the collection of high quality data (see Acknowledgement). These data are used to validate the finite element work that is presented in this paper. Two finite element models are created using commercially available finite element package ANSYS 9.0: a simple soil-arch interaction model and a full bridge model. The simple soil-arch interaction model is mainly used for parametric studies within the service loading range. The material for both arch and soil in the simple soil-arch model is assumed within elastic limit and the interface between the arch and soil is characterised as a friction contact interface. The full bridge model, however, has been created for predicting the failure of the same corresponding experiment. In the full bridge model, the smeared cracking approach is adopted for modelling the masonry behaviour, while the nonlinear behaviour of the soil is simulated with a Drucker-Prager material model. The same friction contact interface is adopted for the full bridge model.

The simple soil-arch interaction model provided a valuable tool for predicting the effect of different parameters on the behaviour of soil-arch interaction. The full bridge model is capable

of reproducing the essential features observed in full scale experiments.

2 NUMERICAL MODELLING APPROACHES FOR MASONRY AND BACKFILL

2.1 Masonry modelling approaches

Masonry is a composite material of bricks and mortar. In general, the approach towards its numerical representation can focus on the micro-modelling of the individual components, or the macro-modelling of masonry as a composite. Unlike masonry material modelling where great interests are in the level of micro-modelling, the modelling methods of masonry arch bridges have mainly concentrated on global aspects rather than on the simulation of its constitutive materials. The current study models the brickwork arches using a macro-modelling approach.

The smeared cracking method is adopted in which the cracking is modelled through an adjustment of material properties which effectively treats the cracking as a “smeared band” of cracks, rather than discrete cracks. The complex behaviour of masonry is assumed to be isotropic before cracking and orthotropic after cracking. Cracking is permitted in three orthogonal directions. A detailed review of the modelling approach has been reported elsewhere (Wang, 2004).

2.2 Backfill modelling approaches

Different constitutive models have been proposed for soil modelling. These constitutive models are essentially pressure-dependent plasticity models. The differences are based on the shape of the yield surface in the meridian plane (either curved or straight meridians, with or without tension cut-off and/or compression cap), the shape of yield surfaces in the deviatoric stress plane (either circular or noncircular yield surfaces), and the use of flow laws (either associated or non-associated flow rules). The choice of the model to be used depends largely on the kind of the material, on the experimental data available for calibration of the model parameters, and on the range of pressure stress values that the material is likely to experience. A brief description of the modelling approach relevant to the current study is discussed here. A more detailed description of different constitutive models and their applicability have been reviewed by Chen et al. (Chen et al. 1990).

The best known failure criterion in soil mechanics is the Coulomb criterion, which is the first type of failure criterion that takes into consideration the effect of the hydrostatic pressure on the strength of granular materials. This criterion states that the resistance to failure of a material is a constant shear strength plus a friction-like force, i.e.

$$\tau = c - \sigma_n \tan \phi \quad (1)$$

where τ is the shear stress, and σ_n is the normal stress (compressive stress as a negative quantity and tensile stress as a positive quantity), c and ϕ are the cohesion and the angle of internal friction, respectively. The Coulomb's failure criterion is an irregular hexagonal pyramid in the principal stress space. The cross-sectional shape of this pyramid on the π -plane is shown in Fig. 1

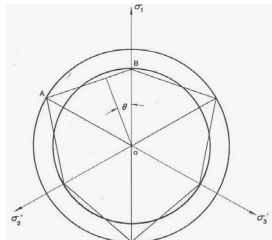


Figure 1 : Drucker-Prager and Coulomb criteria on the π -plane

The Drucker-Prager criterion, formulated in 1952, was a major advance in the extension of metal plasticity to soil plasticity where the influence of a hydrostatic stress component on failure is introduced by inclusion of an additional term I_1 in the von Mises expression.

$$f(I_1, J_2) = \alpha I_1 + J_2 - k = 0 \tag{2}$$

where I_1 is the first invariant of stress tensor, and J_2 is the second invariant of deviatoric stress tensor. α and k are material constants.

The Drucker-Prager criterion can be made to match with the apex of the Coulomb criterion for either point A or B on its π -plane as shown in Fig. 1. For Point A, where the cone circumscribes the hexagonal pyramid (the outer cone), the two surfaces are made to coincide along the compressive meridian (Lode angle = $\pi/3$), and the Drucker-Prager parameters α and k are related to the Coulomb constant c and ϕ by

$$\alpha = \frac{2 \sin \phi}{\sqrt{3}(3 - \sin \phi)}, k = \frac{6c \cos \phi}{\sqrt{3}(3 - \sin \phi)} \tag{3}$$

While for point B (the inner cone) the two surfaces are matched along the tensile meridian (Lode angle = 0), and will have the constants

$$\alpha = \frac{2 \sin \phi}{\sqrt{3}(3 + \sin \phi)}, k = \frac{6c \cos \phi}{\sqrt{3}(3 + \sin \phi)} \tag{4}$$

As the material constants in ANSYS DP model are chosen to match with the compressive meridian of the Coulomb criterion, therefore, the outer cone yield surface is selected. The corresponding yield surface in p - q plane is shown in Fig. 2, where p is the mean stress or hydrostatic stress and q is Mises equivalent deviatoric stress.

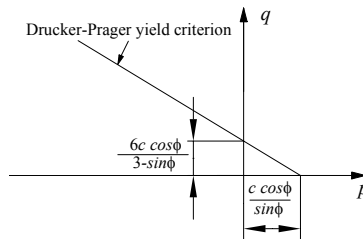


Figure 2 : Drucker-Prager criterion in p - q plane

The flow theory of plasticity is based on three basic assumptions: (1) the existence of an initial yield surface; (2) the evolution of subsequent loading surfaces (hardening rule); (3) the determination of an appropriate flow rule. For the current study, the model is developed using Drucker-Prager material model implement in ANSYS, therefore, the yield surface does not change with progressive yielding, hence there is no hardening rule and the material is assumed elastic - perfectly plastic.

2.3 Contact interface modelling approaches

A variety of numerical approaches have been proposed for the modelling of interface problems. All the methods are essentially attempts to prevent the overlapping of the finite element mesh and to give a satisfactory stress distribution over the contact regions. As the current model is created by ANSYS, a simple frictional contact surface for the soil-arch interface in conjunction with the Augmented Lagrangian method is adopted.

3 SOIL-ARCH INTERACTION FINITE ELEMENT MODEL

In order to validate the approach, a flexible and smooth strip footing on stratum of clay analyzed by Zienkiewicz et al (1975) was re-analysed using Drucker-Prager model implemented in ANSYS. The collapse load predicted by ANSYS DP model using associated flow rule is more than twice that of the load predicted by the Coulomb criterion adopted by Zienkiewicz et al.,. The load predicted by the Coulomb criterion is close to the loads given by the Terzaghi and Prandtl solutions.

As a result, the analysis with the Drucker-Prager material constants matched with the compressive meridian of the Coulomb criterion does not agree with the well-known Terzaghi and Prandtl solutions. It is generally suggested that Drucker-Prager outer cone over-predicts the strength of soil (Griffiths, 1990). Therefore, the selection of the material constants using the Drucker-Prager criterion is critical.

3.1 Simple soil-arch interaction model

3.1.1 Geometry and model

The geometry of the simple soil-arch interaction model is shown in Fig. 3. The arch is of 3m span with span to rise ratio of 4:1. The thickness of the arch ring is 215mm. The geometry of soil is control by SSSL, SLSL and h_{soil} (see Fig. 3). The arch and soil were both modelled using SOLID45 (8-node solid element), while contact element CONTACT173 and target element TARGET170 (4-node interface elements) are used for modelling the interface between soil and arch barrel interface. A typical meshed simple soil-arch interaction model is shown in Fig. 4.

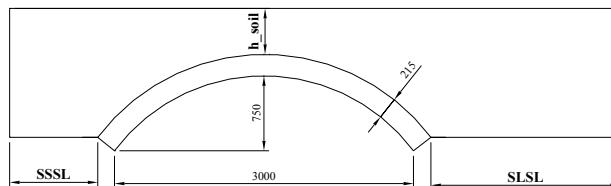


Figure 3 : Geometry of simple soil-arch interaction model

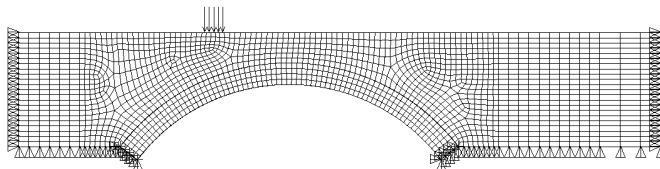


Figure 4 : FE mesh, loading and boundary condition for simple soil-arch interaction model

3.1.2 Boundary condition and loading

The boundary condition for the simple soil-arch interaction model is shown in Fig. 4. The arch barrel was fixed at both supports, and the plain strain condition is assumed for the soil.

A vertical patch load (width of 219mm) was applied at the quarter span position and the maximum applied pressure 0.3N/mm^2 is determined by controlling the maximum tensile stress in the arch barrel which is no greater than the assumed tensile strength of the material (0.5N/mm^2 based on previous experimental data for similar brickwork arches (see Melbourne et al. 2007).

3.1.3 Material

The material properties for the arch and the soil are given in Table 1. The coefficient of friction for the interface is assumed to be 0.7 except for the study of the influence of this parameter (varies from 0.3 to 0.9).

Table 1 : Material properties for simple soil-arch model

		Arch barrel	soil
Young's modulus	N/mm ²	16000	1000*
Poisson's Ratio		0.2	0.2
Density	Kg/ m ³	2200	2000

*varies from 200 to 10000N/mm² for relative stiffness studies

3.1.4 Results and discussion

3.1.4.1 The influence of the geometry of the soil

Fig. 5 shows the influence of SSSL, SLSL and the depth of fill above the crown (h_{soil}) on the maximum tensile principal stress in the intrados of the arch barrel (S_{1max}), and the maximum von Mises stress (SEQV) in the soil.

The influence of the horizontal extent of the soil on both side of the supports on stress and displacement is generally insignificant especially when they are over 1m. This indicates that at this level of loading, only the soil immediately surrounding the arch barrel has interacted with the arch barrel. The rest of the studies are based on SSSL = 1m and SLSL = 2m.

The influence of the depth of fill above the crown on the maximum tensile principal stress in the arch barrel is significant. When the fill cover approaches 1.2m the model predicts that it is unlikely for the arch barrel to crack before the yielding of the soil. It also suggests that when there is sufficient fill cover, the load can be dispersed directly to the base of the soil.

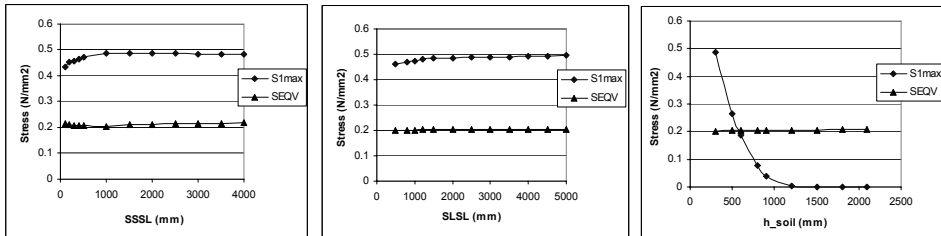


Figure 5 : Influence of the geometry of the soil

3.1.4.2 The influence of relative stiffness of arch barrel to the soil

The influence of the relative stiffness of arch barrel to the soil is studied by keeping the Young's modulus of the arch constant ($E_{arch}=16000N/mm^2$) and varying the Young's modulus of the soil (E_{soil}) from 200 to 10000N/mm². The influence on stress in arch barrel and soil is shown in Fig. 6.

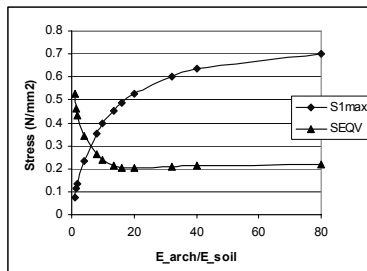


Figure 6 : Influence of relative stiffness between arch barrel and soil

The influence of relative stiffness is clearly very significant not only on the value of the maximum stresses but also on the positions of where these stresses occur. For most case (except for the $E_{ratio} < 4$), the maximum tensile stress occurs in the intrados of the arch barrel indicating that if the same yield criteria is used for both soil and arch, the yielding or cracking will initiated from the arch barrel intrados.

3.1.4.3 The influence of contact stiffness on soil arch interface

Special care should be taken when selecting the values of contact stiffness between arch barrel and soil interface. Normal contact stiffness is used to enforce compatibility between the contact surfaces. If the contact stiffness factor (KFN) is too small, the amount of penetration of contact surface into target surface may be too great resulted in fictitious soft interface and the solution can be incorrect. On the other hand, if the stiffness is too big, the determination of the true contact status normally requires more iterations, and in some cases, convergence difficulties are inevitable.

The study has shown that the normal contact stiffness factor of 0.1 gives reasonable stress levels in the arch barrel and prevent overlapping between interfaces (penetration smaller than 0.1mm), it also leads to efficient solutions in terms of the number of iterations.

3.1.4.4 The influence of mesh density

The art of using the finite element method lies in an appropriate mesh density to solve a problem. If the mesh is too coarse then the inherent element approximations will not allow a correct solution to be obtained. Alternatively, if the mesh is too fine the cost of the analysis can be out of proportion to the results obtained. It is therefore important to use a sufficiently refined mesh to ensure that the results from FE simulation are adequate.

As far as the deflection is concerned even a coarse mesh will result in easy convergence. For the convergence of stress, at least four elements are need across the thickness of the arch barrel. For the maximum principal stress at an integration point, the convergence is much slower and the difference between stress from integration point and stress extrapolating from integration point always exists even with a finer mesh (more than eight elements across the thickness). Mesh sensitivity will, therefore, exist when cracking is based on the stress at integration points. The rest of the studies are based on four elements across the thickness of the arch barrel.

3.1.4.5 The influence of abutment fixity and soil boundary conditions

The influence of the boundary condition on the bottom face of the soil is studied by changing from perfectly smooth and rigid to perfectly rough and rigid. The influence on the maximum displacement and the stress level in both arch barrel and soil is shown in Table 2.

Table 2 : influence of soil boundary condition

Soil bottom face boundary conditions	S1max N/mm ²	USUM mm	SEQV N/mm ²
Perfectly smooth and rigid	0.4863	0.2389	0.2029
Perfectly rough and rigid	0.4762	0.2336	0.2038

Table 3 : influence of abutment fixity

abutment boundary conditions	S1max N/mm ²	USUM mm	SEQV N/mm ²
Both sides fixed	0.4863	0.2389	0.2029
Both sides free to move horizontally	1.327	0.4104	0.2094

The influence of the soil boundary condition within elastic range of loading is not as significant as the abutment fixity of the arch barrel, see Table 3.

Although the maximum horizontal movement on both side is less than 0.2mm at the current load level, the maximum principal stress in the arch barrel has nearly tripled, and the position of

the stress has moved from quarter span intrados to the extrados of left-hand abutment, which indicates that the crack will start from here rather than the quarter span intrados.

3.2 Full bridge models

In order to study the fixity conditions of abutments, two full bridge models are created: one with abutments comprised top and bottom parts, the other with the same size but only comprised one part for each abutment.

3.2.1 Geometry and model

The geometry of the full bridge model is shown in Fig. 7, based on the experimental data reported by Gilbert et al. (Gilbert et al. 2006) and <http://www.sustainablebridges.net> (SB4.7.1, 2007).

The arch was modelled using 8-node solid element with cracking and crushing capabilities, while the soil was modelled using the same element but with Drucker-Prager properties. The same interface elements as the simple soil-arch model are used for the full bridge models.

A typical meshed simple soil-arch interaction model is shown in Fig. 8.

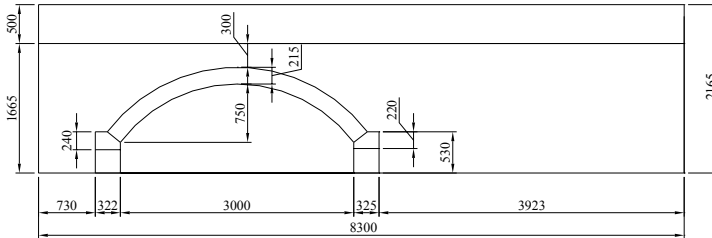


Figure 7 : Geometry of full bridge model

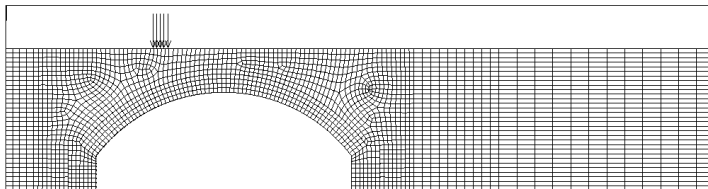


Figure 8 : FE mesh, loading for full bridge model

3.2.2 Boundary condition and loading

The boundary condition for the full bridge model was similar to that of simple soil-arch interaction model except the soil was constrained by a rigid tank which is fixed in all directions. The lower section of the abutments were fixed at the bottom face. A vertical patch load (width of 219mm) was applied at quarter span position.

3.2.3 Material

The material properties for arch and soil are given in Table 4. The coefficient of friction for the interface of top and bottom abutment is 0.7 (based on the laboratory data), and 0.01 for the rigid tank and soil interface. The initial study assumes a friction coefficient of 0.7 for the rest of soil-structure interfaces.

Table 4 : material properties for full bridge model

		Arch barrel	soil
Young's modulus	N/mm ²	16000	1000
Poisson's Ratio		0.2	0.2
Density	Kg/ m ³	2200	1910
Uniaxial tensile cracking stress	N/mm ²	0.48	
Uniaxial compressive stress	N/ mm ²	24	
Cohesion	N/ mm ²		0.0224
Internal angle of friction	degree		46.4

3.2.4 Results and discussion

Fig. 9 shows the displacement vector from the FE full bridge model when all the cracks have occurred in the arch barrel. The arch failed by the formation of 'hinged' mechanism plus the sliding between top and bottom parts of the abutments. All these essential features are similar to the large-scale bridge test.

Initial study has shown that the maximum load predict from the FE model is very sensitive to the material properties such as cohesion, angle of friction, dilatancy, tensile strength of the brickwork, density and relative stiffness between brickwork and soil. If associated flow rule is adopted and the same material properties described in 3.2.3 are used, the maximum load predicted by the same FE model is 2.7 times higher than that using non-associated flow rule. The latter is 1.3 times of the experimental result. Therefore, interpretation of these parameters from lab tests is critical.

The parametric study is forming part of the ongoing research programmes and will be reported elsewhere in due course.

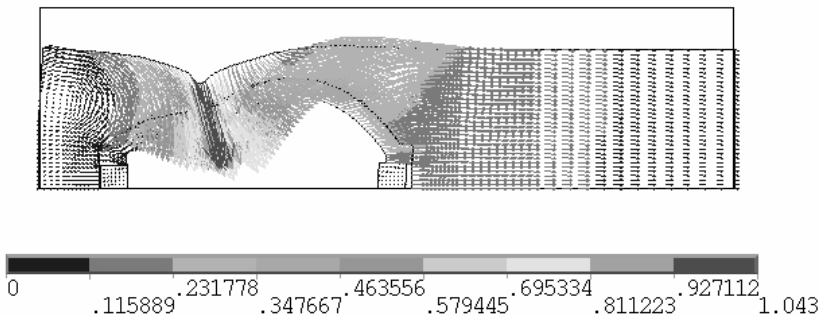


Figure 9 : Displacement vector after all the crack occurred (P=164kN/m)

4 CONCLUSIONS

The following conclusions can be drawn from the current finite element analyses:

- Under the service load level, the soil-arch interaction is limited only to the soil immediately surrounding the arch barrel;
- The relative stiffness of the arch and the soil is a very important factor on soil-arch interaction;
- The fixity of the abutments affect the load at which the 1st crack occurs and will in turn affect the load redistribution in the bridge;
- The full bridge model can predict the essential feature observed in full scale experiments;
- The load carrying capacity from the FE model is very sensitive to the material properties like density, cohesion of soil, the internal angle of friction, dilatancy and the tensile strength of the brickwork.

ACKNOWLEDGEMENT

The authors acknowledge the financial support provided by EU Framework VI project ‘Sustainable Bridges’, EPSRC, Network Rail, Essex County Council, and the collaboration with Sheffield University.

REFERENCES

- Chen, W.F. and E. Mizuno. 1990. *Non-linear Analysis in Soil Mechanics – Theory and Implementation*. The Netherlands: Elsevier Science Publishers B.V.
- Gilbert, M. Smith, C.C., Melbourne, C and Wang, J 2006. An experimental study of soil-arch interaction in masonry bridges. IABMAS'06 - Third International Conference on Bridge Maintenance, Safety and Management
- Griffiths, D. V. 1990. Failure criterion interpretation based on Mohr-Coulomb friction, *J. Geotech. Engng.* ASCE, 116, p. 986-999
- Melbourne, C. Wang, J. and Tomor, A. K. 2007. New Masonry Arch Bridge Assessment Strategy (SMART), accepted for publication in the Bridge Engineering Journal in June 07.
- SB4.7.1. Structural assessment of masonry arch bridges. Background document D4.7.1 to “Guideline for Load and Resistance Assessment of Railway Bridges”. Prepared by Sustainable Bridges- a project within EU FP6. 2007. Available from: www.sustainablebridges.net.
- Wang, J. 2004. The Three dimensional Behaviour of Masonry Arches, PhD thesis, University of Salford,
- Zienkiewicz, O. C., Humpheson, C. and Lewis, R. W., 1975. Associated and non-associated viscoplasticity and plasticity in soil mechanics. *Geotechnique*, 25 (4), p. 671-689

